



**HAL**  
open science

## How could 50°C be reached in Paris: analysing the CMIP6 ensemble to design storylines for adaptation

Pascal Yiou, Robert Vautard, Yoann Robin, Nathalie N. de Noblet-Ducoudré,  
Fabio d'Andrea, Robin Noyelle

### ► To cite this version:

Pascal Yiou, Robert Vautard, Yoann Robin, Nathalie N. de Noblet-Ducoudré, Fabio d'Andrea, et al.. How could 50°C be reached in Paris: analysing the CMIP6 ensemble to design storylines for adaptation. Climate services, In press. hal-04525038v2

**HAL Id: hal-04525038**

**<https://hal.science/hal-04525038v2>**

Submitted on 17 Sep 2024

**HAL** is a multi-disciplinary open access archive for the deposit and dissemination of scientific research documents, whether they are published or not. The documents may come from teaching and research institutions in France or abroad, or from public or private research centers.

L'archive ouverte pluridisciplinaire **HAL**, est destinée au dépôt et à la diffusion de documents scientifiques de niveau recherche, publiés ou non, émanant des établissements d'enseignement et de recherche français ou étrangers, des laboratoires publics ou privés.

# How could 50°C be reached in Paris: Analyzing the CMIP6 ensemble to design storylines for adaptation

Pascal Yiou (1), Robert Vautard (1), Yoann Robin (1), Nathalie de Noblet-Ducoudré (1), Fabio D'Andrea (2), Robin Noyelle (1)

(1) Laboratoire des Sciences du Climat et de l'Environnement, UMR8212 CEA-CNRS-UVSQ, IPSL & Université Paris-Saclay, 91191 Gif-sur-Yvette, France

(2) Laboratoire de Météorologie Dynamique, UMR CNRS-X-ENS, IPSL & Université PSL, 75005 Paris, France

## Keywords

Heatwaves, CMIP6, Model selection, Paris

## Abstract

Reaching a surface temperature of 50°C in a heavily populated region, like Paris, would have devastating effects. Although such a high value seems far from the present-day record of 42.6°C, its occurrence cannot be dismissed by the end of the 21<sup>st</sup> century, due to the continuous increase of global mean temperature. In this paper, we address two questions that were asked by the City of Paris to a group of scientists: When does this event start to be likely? What are the prevailing meteorological conditions? We base our study on the CMIP6 simulation ensemble. Many of the CMIP6 yield biases in temperature. Rather than using methods of bias correction, which are not necessarily adapted to high extremes, we propose a pragmatic approach of model selection in order to seek such high temperature events that are deemed realistic. We analyze the meteorological conditions leading to first occurrences of such hot events and their common atmospheric patterns. This paper describes a simple data mining approach (on a large ensemble of climate model simulations) which could be adapted to other regions of the world, in order to help decision makers anticipating and adapting to such devastating meteorological events.

## 1 Practical implications

The present study came as a request from the City of Paris, who was interested in the meteorological conditions that would prevail if such high temperatures were reached in Paris. The City of Paris worries, in case of extreme heat in the city, about its capacity to maintain the distribution of water and energy, to carry out emergency procedures such as ambulances,

1 welcome people to the emergency room in hospitals, extinguish starting fires, protect elderly  
2 people, and welcome children at school in good conditions. Thus, the City of Paris wanted to  
3 set up ad hoc organizational changes prior to reaching such high temperature levels  
4 ([https://cdn.paris.fr/paris/2023/04/21/paris\\_a\\_50\\_c-le\\_rapport-Jc4H.pdf](https://cdn.paris.fr/paris/2023/04/21/paris_a_50_c-le_rapport-Jc4H.pdf)). Implementing the  
5 work to identify the risks of malfunctioning and to propose adaptation solutions is costly (in  
6 time, money and energy). The authors of this paper were solicited to first establish whether  
7 such high temperatures could occur in Paris and in which climatic conditions. Once they  
8 validated that 50°C in Paris could occur if the global warming level exceeds 2°C, stress tests  
9 were carried out in some Paris districts in October 2023. Although the City of Paris did not use  
10 the exact numbers we produced in this study (e.g., year of occurrence), explaining that such  
11 an event could occur during the course of our lifetimes increased the awareness of the public  
12 by making it more concrete.

13 The “real life” stress test findings revealed that to be more resilient, the City of Paris needs to  
14 act and invest urgently to lower the temperature impacts of the heat hazard (e.g., with a  
15 better water and vegetation management), and the impacts on population (though better  
16 monitoring). A resilience plan for Paris is in construction, that gathers all the stakeholders  
17 (urban management, water management, health, police). Therefore, the work reported in this  
18 paper supports investments to identify the risks of “domino” failures when too many  
19 solicitations load the emergency system and to implement a series of adaptation processes to  
20 get ready when such an event occurs [[https://www.paris.fr/pages/paris-50-c-un-exercice-  
21 grandeur-nature-pour-se-preparer-aux-chaleurs-extremes-24322,](https://www.paris.fr/pages/paris-50-c-un-exercice-grandeur-nature-pour-se-preparer-aux-chaleurs-extremes-24322)  
22 [https://www.lemonde.fr/planete/article/2022/07/16/comment-paris-se-prepare-a-vivre-  
23 sous-50-c\\_6135001\\_3244.html](https://www.lemonde.fr/planete/article/2022/07/16/comment-paris-se-prepare-a-vivre-sous-50-c_6135001_3244.html)]. Other French cities like Perpignan (South of France), which  
24 are likely to witness such high temperatures before Paris does, are also interested in such  
25 diagnostics [[https://madeinperpignan.com/evenement-perpignan-50-degres-climat-eau-  
26 biodiversite/](https://madeinperpignan.com/evenement-perpignan-50-degres-climat-eau-biodiversite/)].

27 Even though the computations presented in this paper are conceptually simple, they require  
28 extensive computing power and handling complex file formats. If such a study was to be  
29 reproduced for other regions or cities, this work could be left to “intermediate entities” (e.g.,  
30 small and medium enterprises: SMEs) who could use the suite of scripts that we provide on  
31 github. Therefore, if data mining for extreme events has an economic value, we present and  
32 document tools to achieve it. A French start-up SME is presently working on ways to optimize  
33 computations.

## 34 2 Introduction

35 Heatwaves have huge impacts on society and ecosystems (Bastos et al., 2020; Domeisen et  
36 al., 2023; Yin et al., 2023), and frequently generate thousands of extra deaths per summer in  
37 Europe. Western European governments took measures to lower vulnerability, after the  
38 European heatwaves in 2003. The Pacific North West American heat wave in June 2021 was a  
39 shock with temperatures that came close to 50°C during a couple of days, and were way above  
40 previous historical records (Philip et al., 2022). The authorities of a few major cities (in  
41 particular in Europe) are in the process of designing adaptation plans to such events, yet  
42 unprecedented in Europe, where records since 1950 reach 40-45°C, except for a few  
43 Mediterranean cities (Athens, Syracuse, Cordoba), with record nearing or exceeding 48°C.

44 There is no universal definition of a heatwave. In France, Météo France defines a heatwave  
45 when day and night temperatures exceed a high threshold (that depends on the region) for  
46 more than 3 consecutive days. For safety purposes, *heatwave warnings* can be issued when

1 temperatures can exceed high thresholds, even for short durations. For the Paris area, the  
2 threshold values for a “red” warning (leading to conditions similar to those of the summer  
3 2003) are 31°C during day time (daily maximum temperature: TX) and 21°C at night (daily  
4 minimum temperature: TN) (Dangé, 2023). Therefore, there are distinct notions of heat: one  
5 is based on the persistence of high temperatures, and the other (which triggers warnings) is  
6 based on the intensity only. This paper will focus on the latter.

7 The city of Paris, with a record (2019) of 42.6°C, is preparing an adaptation plan to extreme  
8 summer temperatures, and a crisis plan for temperatures in the range of 50°C (Florentin and  
9 Lelievre, 2023). Scientific questions that have been asked to the (French) scientific community  
10 are:

- 11 1. Can temperatures exceed 50°C in Paris and for how long?
- 12 2. What is a likely horizon for the first occurrence of such an event?
- 13 3. How are the 50°C reached?

14 The record shattering event across Western Canada and the US in 2021 (i.e., at a similar  
15 latitude as the Paris area) suggests that one could not dismiss that such a hot event could  
16 occur in Europe in years/decades to come. Such temperatures were also observed in southern  
17 Europe in 2021 and 2023. Therefore, preparing a crisis exercise and adaptation plans for that  
18 level of temperatures is important now, as adaptation actions will take time to be effective.

19 When daily temperature records are broken, the increments above the previous record are  
20 generally a few tenths of degrees. In the Pacific NorthWest American event in summer in 2021,  
21 this was called a “record shattering” event because records were broken by several degrees  
22 (Fischer et al., 2021). Such record shattering events can be seen as outliers of observed  
23 extreme value distributions (Fischer et al., 2023), and hence can be qualified as surprises.  
24 Using data from 1950, Philip et al. (2022) estimated a return period for the event of the order  
25 of about 1000 year, accounting for the current global warming level. (Bador et al., 2017) have  
26 investigated temperature records in regional climate projections. Based on a single climate  
27 model, they found the possibility to exceed locally 50°C in France but not in the Paris region.  
28 Here we are interested in hot events that would occur as surprises, similarly to the recent  
29 events of 2021 or 2023. Such events are deemed to have a low probability (Philip et al., 2022),  
30 which requires large ensemble of data (Bevacqua et al., 2023).

31  
32 The objective of this article is to present a method that allows analyzing the possibility of  
33 temperatures to reach 50°C in the Paris and provide physically plausible example cases which  
34 can serve city managers and planners for adaptation reference using recent climate  
35 projections. The recent CMIP6 simulations offer a large multi-model ensemble of data, with  
36 several socio-economic scenarios until the end of the 21<sup>st</sup> century.

37 This paper also aims at succinctly describing the conditions under which temperatures of 50°C  
38 can be reached in a highly populated European region like Ile-de-France, surrounding Paris  
39 (France). We examine the large-scale atmospheric conditions for such an event, and the global  
40 warming level above which such conditions are found with significant probabilities in the  
41 simulations, accounting for the interannual and interdecadal variability. We mainly describe a  
42 data processing chain, and defer a complete physical analysis to another paper.

43  
44 This description can lead to a *climate service*, to analyze a large ensemble of climate  
45 simulations, and provide sensible answers to the challenges outlined in this introduction (Is it  
46 possible to reach 50°C? When? What climatic and meteorological conditions to expect?). The  
47 goal is to be able to replicate our analyses easily and change parameters, so that the

1 computations can be transposed to other regions of the planet. Although those data are  
 2 publicly available, their volume is huge (peta-bytes of data). Treating an ensemble such as  
 3 CMIP6 requires scientific computer skills and R&D resources, which are rarely available from  
 4 city practitioners whose main interest is not atmospheric sciences. It is hence deemed useful  
 5 to propose a simple methodology, easily reproducible by companies providing consulting or  
 6 climate services, to treat the three challenges outlined above from available data. Hence, this  
 7 processing chain is intended for entities that are capable of processing climate model data,  
 8 and communicate results to final stakeholders. To potentially become useful for other cities,  
 9 such a methodology should be easy to deploy, reproducible and testable on many regions. We  
 10 however restrict here to the Paris city for the presentation.

11  
 12 Section 2 presents data and models used in this paper. Section 3 describes the first three  
 13 events that reach 50°C in the Paris area in three SSP scenarios. This section presents a quick  
 14 check of the atmospheric conditions that prevail during those events. Section 4 discusses the  
 15 caveats of the analyses. Section 5 explains practical implications of this paper and how the  
 16 City of Paris used some of the results. The paper concludes with Section 6.

## 17 3 Data and methods

### 18 3.1 Data

19 This analysis uses E-OBS data (Haylock et al., 2008), ERA5 reanalyses (Hersbach et al., 2020)  
 20 and CMIP6 simulations (Eyring et al., 2016). The CMIP6 simulations include “historical” and  
 21 four Shared Socioeconomic Pathway (SSP) scenarios (Riahi et al., 2017): 1-2.6, 2-4.5, 3-7.0 and  
 22 5-8.5. Historical simulations run from 1860 to 2014, and are constrained by observed forcings  
 23 (natural and anthropogenic). SSP simulations go from 2015 to 2100 (2300 for some models)  
 24 and are constrained by economic scenarios of greenhouse gas emissions, pollutants and  
 25 changes in land use.

26 Some models provide ensembles of simulations, with slightly perturbed initial conditions. This  
 27 helps assessing the role of internal climate variability (Deser et al., 2016).

28 Overall, we considered all simulations that were available to us on August 1<sup>st</sup> 2023 on the IPSL  
 29 computing server, which contains a (large) subset of the simulations on the Earth System Grid  
 30 Federation (ESGF) that contains all CMIP6 simulations. We used the models for which  
 31 historical runs and the four SSP scenarios are available. This includes 1288 simulations from  
 32 26 climate models. Hence this excludes models with fewer scenario simulations. The ensemble  
 33 sizes for each model (with historical and four SSP scenario simulations) are indicated in Table  
 34 1 below. The ensemble sizes vary from 1 run to more than 50 in SSP simulations, depending  
 35 on the model. The size of the ensembles also depends on the SSP scenarios.

36

| Model                | Scenario   | Ensemble size | Model     | Scenario   | Ensemble size |
|----------------------|------------|---------------|-----------|------------|---------------|
| <b>ACCESS-CM2</b>    | historical | 10            | GFDL-ESM4 | historical | 3             |
| <b>ACCESS-CM2</b>    | ssp126     | 3             | GFDL-ESM4 | ssp126     | 1             |
| <b>ACCESS-CM2</b>    | ssp245     | 3             | GFDL-ESM4 | ssp245     | 1             |
| <b>ACCESS-CM2</b>    | ssp370     | 3             | GFDL-ESM4 | ssp370     | 1             |
| <b>ACCESS-CM2</b>    | ssp585     | 5             | GFDL-ESM4 | ssp585     | 1             |
| <b>ACCESS-ESM1-5</b> | historical | 40            | INM-CM4-8 | historical | 1             |
| <b>ACCESS-ESM1-5</b> | ssp126     | 10            | INM-CM4-8 | ssp126     | 1             |
| <b>ACCESS-ESM1-5</b> | ssp245     | 18            | INM-CM4-8 | ssp245     | 1             |
| <b>ACCESS-ESM1-5</b> | ssp370     | 10            | INM-CM4-8 | ssp370     | 1             |

|                         |            |    |                      |            |    |
|-------------------------|------------|----|----------------------|------------|----|
| <b>ACCESS-ESM1-5</b>    | ssp585     | 40 | INM-CM4-8            | ssp585     | 1  |
| AWI-CM-1-1-MR           | historical | 5  | INM-CM5-0            | historical | 10 |
| AWI-CM-1-1-MR           | ssp126     | 1  | INM-CM5-0            | ssp126     | 1  |
| AWI-CM-1-1-MR           | ssp245     | 1  | INM-CM5-0            | ssp245     | 1  |
| AWI-CM-1-1-MR           | ssp370     | 5  | INM-CM5-0            | ssp370     | 5  |
| AWI-CM-1-1-MR           | ssp585     | 1  | INM-CM5-0            | ssp585     | 1  |
| BCC-CSM2-MR             | historical | 3  | <b>IPSL-CM6A-LR</b>  | historical | 33 |
| BCC-CSM2-MR             | ssp126     | 1  | <b>IPSL-CM6A-LR</b>  | ssp126     | 6  |
| BCC-CSM2-MR             | ssp245     | 1  | <b>IPSL-CM6A-LR</b>  | ssp245     | 11 |
| BCC-CSM2-MR             | ssp370     | 1  | <b>IPSL-CM6A-LR</b>  | ssp370     | 11 |
| BCC-CSM2-MR             | ssp585     | 1  | <b>IPSL-CM6A-LR</b>  | ssp585     | 7  |
| CAMS-CSM1-0             | historical | 1  | KACE-1-0-G           | historical | 3  |
| CAMS-CSM1-0             | ssp126     | 1  | KACE-1-0-G           | ssp126     | 3  |
| CAMS-CSM1-0             | ssp245     | 1  | KACE-1-0-G           | ssp245     | 3  |
| CAMS-CSM1-0             | ssp370     | 1  | KACE-1-0-G           | ssp370     | 3  |
| CAMS-CSM1-0             | ssp585     | 1  | KACE-1-0-G           | ssp585     | 3  |
| <b>CanESM5</b>          | historical | 50 | <b>MIROC-ES2L</b>    | historical | 31 |
| <b>CanESM5</b>          | ssp126     | 50 | <b>MIROC-ES2L</b>    | ssp126     | 3  |
| <b>CanESM5</b>          | ssp245     | 50 | <b>MIROC-ES2L</b>    | ssp245     | 30 |
| <b>CanESM5</b>          | ssp370     | 50 | <b>MIROC-ES2L</b>    | ssp370     | 1  |
| <b>CanESM5</b>          | ssp585     | 50 | <b>MIROC-ES2L</b>    | ssp585     | 2  |
| <b>CMCC-ESM2</b>        | historical | 1  | MIROC6               | historical | 50 |
| <b>CMCC-ESM2</b>        | ssp126     | 1  | MIROC6               | ssp126     | 50 |
| <b>CMCC-ESM2</b>        | ssp245     | 1  | MIROC6               | ssp245     | 50 |
| <b>CMCC-ESM2</b>        | ssp370     | 1  | MIROC6               | ssp370     | 3  |
| <b>CMCC-ESM2</b>        | ssp585     | 1  | MIROC6               | ssp585     | 50 |
| CNRM-CM6-1              | historical | 30 | <b>MPI-ESM1-2-HR</b> | historical | 10 |
| CNRM-CM6-1              | ssp126     | 1  | <b>MPI-ESM1-2-HR</b> | ssp126     | 2  |
| CNRM-CM6-1              | ssp245     | 1  | <b>MPI-ESM1-2-HR</b> | ssp245     | 2  |
| CNRM-CM6-1              | ssp370     | 3  | <b>MPI-ESM1-2-HR</b> | ssp370     | 10 |
| CNRM-CM6-1              | ssp585     | 1  | <b>MPI-ESM1-2-HR</b> | ssp585     | 2  |
| CNRM-ESM2-1             | historical | 10 | MPI-ESM1-2-LR        | historical | 31 |
| CNRM-ESM2-1             | ssp126     | 1  | MPI-ESM1-2-LR        | ssp126     | 10 |
| CNRM-ESM2-1             | ssp245     | 1  | MPI-ESM1-2-LR        | ssp245     | 10 |
| CNRM-ESM2-1             | ssp370     | 3  | MPI-ESM1-2-LR        | ssp370     | 10 |
| CNRM-ESM2-1             | ssp585     | 1  | MPI-ESM1-2-LR        | ssp585     | 30 |
| <b>EC-Earth3</b>        | historical | 73 | <b>MRI-ESM2-0</b>    | historical | 12 |
| <b>EC-Earth3</b>        | ssp126     | 2  | <b>MRI-ESM2-0</b>    | ssp126     | 1  |
| <b>EC-Earth3</b>        | ssp245     | 30 | <b>MRI-ESM2-0</b>    | ssp245     | 9  |
| <b>EC-Earth3</b>        | ssp370     | 52 | <b>MRI-ESM2-0</b>    | ssp370     | 5  |
| <b>EC-Earth3</b>        | ssp585     | 58 | <b>MRI-ESM2-0</b>    | ssp585     | 5  |
| <b>EC-Earth3-Veg</b>    | historical | 9  | NorESM2-LM           | historical | 3  |
| <b>EC-Earth3-Veg</b>    | ssp126     | 5  | NorESM2-LM           | ssp126     | 1  |
| <b>EC-Earth3-Veg</b>    | ssp245     | 6  | NorESM2-LM           | ssp245     | 3  |
| <b>EC-Earth3-Veg</b>    | ssp370     | 4  | NorESM2-LM           | ssp370     | 3  |
| <b>EC-Earth3-Veg</b>    | ssp585     | 8  | NorESM2-LM           | ssp585     | 1  |
| <b>EC-Earth3-Veg-LR</b> | historical | 3  | <b>NorESM2-MM</b>    | historical | 3  |
| <b>EC-Earth3-Veg-LR</b> | ssp126     | 3  | <b>NorESM2-MM</b>    | ssp126     | 1  |

|                         |            |   |                   |            |   |
|-------------------------|------------|---|-------------------|------------|---|
| <b>EC-Earth3-Veg-LR</b> | ssp245     | 3 | <b>NorESM2-MM</b> | ssp245     | 2 |
| <b>EC-Earth3-Veg-LR</b> | ssp370     | 3 | <b>NorESM2-MM</b> | ssp370     | 1 |
| <b>EC-Earth3-Veg-LR</b> | ssp585     | 3 | <b>NorESM2-MM</b> | ssp585     | 1 |
| FGOALS-g3               | historical | 5 | TaiESM1           | historical | 1 |
| FGOALS-g3               | ssp126     | 4 | TaiESM1           | ssp126     | 1 |
| FGOALS-g3               | ssp245     | 4 | TaiESM1           | ssp245     | 1 |
| FGOALS-g3               | ssp370     | 5 | TaiESM1           | ssp370     | 1 |
| FGOALS-g3               | ssp585     | 4 | TaiESM1           | ssp585     | 1 |

1  
2 *Table 1: List of CMIP6 models and ensemble sizes for each scenario that are treated in this paper. We only indicate the models*  
3 *for which historical and four SSP scenario runs are available. We excluded the models based on the Met Office Hadley Center*  
4 *(MOHC) model simulations, as they yield documented anomalous behavior for TX. The models in boldface characters are those*  
5 *which pass the Kolmogorov-Smirnov test of a comparison with ERA5 and E-OBS data.*

6  
7 We considered TX (daily maximum temperature), TG (daily mean temperature) and TN (daily  
8 minimum temperature) over France, and SLP (sea-level pressure) over the North Atlantic  
9 region, in order to investigate the synoptic conditions during heat events in Paris.

10 In the selection of models, we removed simulations of the HadGEM3-GC31-HH, HadGEM3-  
11 GC31-HM, HadGEM3-GC31-LL, HadGEM3-GC31-LM, HadGEM3-GC31-MH, HadGEM3-GC31-  
12 MM, and UKESM1-0-LL models. For those models, the errata documentation for CMIP6 states  
13 that: “An issue has been discovered where isolated and irregular events are leading to spikes  
14 (a single time step) in the value of surface air temperature lead to the value of daily tasmax<sup>1</sup>  
15 datasets in all MOHC simulations that include the atmosphere. Initial investigations on a single  
16 simulation suggest that events over 340K occur once in every 250 days, with events above  
17 350K occurring once in every 1,200 days. We believe the spikes in tasmax are triggered by the  
18 model’s surface energy balance, at isolated grid cells, being dominated by sensible heating.  
19 For very short periods the accumulated heat appears not to be efficiently mixed away from  
20 the surface by the model’s sub-grid scale mixing scheme resulting in the spurious values [...]”.  
21 (<https://errata.ipsl.fr/static/view.html?uid=76b3f818-d65f-c76b-bfd8-cae5bc27825c>). We  
22 checked that the other models we consider do not have such documented issues on  
23 temperature.

24  
25 We extracted TX, TN and TG over the Paris region (Ile de France) outlined in Figure 1. A bilinear  
26 interpolation was performed on the model grid cells over the [1.75-3.25°E; 48.25-49.25°N]  
27 region, which includes the administrative area of the City of Paris. This interpolation procedure  
28 is necessary because Ile de France can be across several model gridcells, whose size can be  
29 much larger (~2°) than the area of the region itself. When the spatial average across the region  
30 is computed, this interpolation allows weighting the model grid cell that cover the Ile de  
31 France region. We note that this computation takes ~28h (for each variable) on the IPSL  
32 computing cluster, using 8 parallel CPUs.

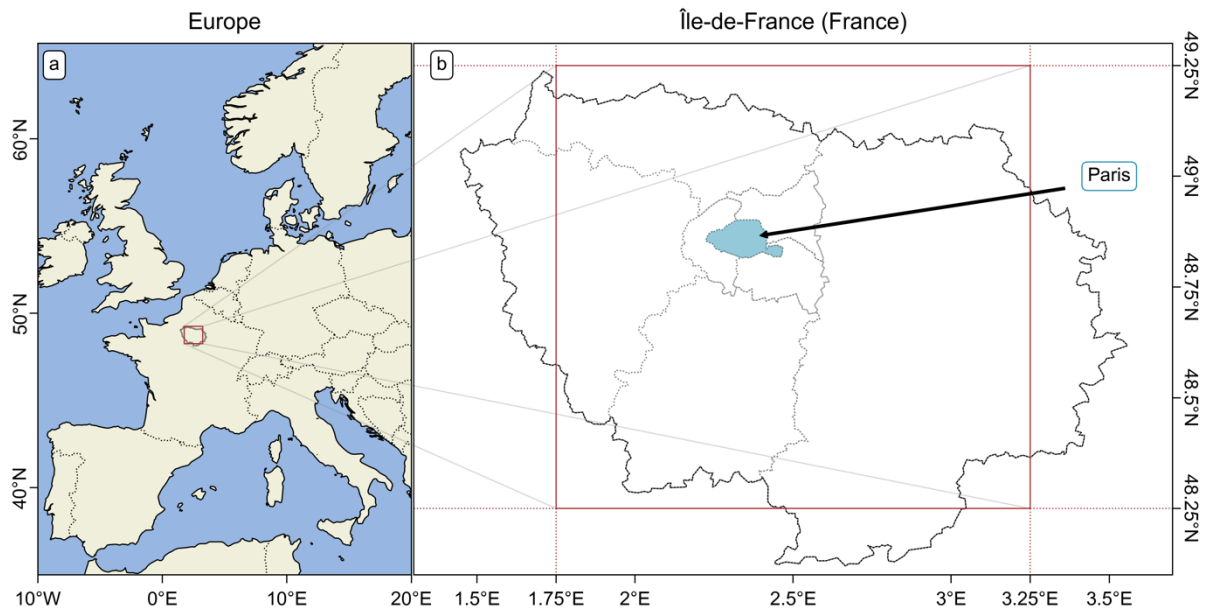
33  
34 We computed the yearly global mean surface temperature (GMST) for each CMIP6 model. The  
35 GMST value between 1950 and 2000 is around ~14.1 +/- 0.5°C (1 sigma) for the CMIP6  
36 historical simulations. The mean GMST in ERA5 for these decades is ~13.5°C. We determine

<sup>1</sup> Tasmax is equivalent to TX. The citation is reproduced verbatim.



1 global warming increase (GWI) as the difference of a 20-year average GMST with the average  
 2 value at the turn of the 21<sup>st</sup> century (1950-2000) or at the turn of the 20<sup>th</sup> century (1850-1900).  
 3 The latter baseline (from a pre-industrial period) is often used in IPCC reports (IPCC, 2021). In  
 4 practice, there are three caveats to such a baseline definition: (i) some historical simulations  
 5 provided on the ESGF servers start in the 20<sup>th</sup> century, (ii) reanalysis products like ERA5  
 6 (Hersbach et al., 2020) or NCEP (Kalnay et al., 1996) start after 1948, which makes data  
 7 validation difficult, and (iii) a large majority living humans (incl. decision makers) were born  
 8 after 1950, so that communication from a known baseline is certainly more meaningful.  
 9 Therefore, we will focus on a definition of “global warming” from a 1950-2000 baseline.  
 10 A generic code for extracting time series over a given region from the whole CMIP6 archive is  
 11 provided on github [<https://github.com/pascalgiou/Paris50C.git>].  
 12

13 We also used TG from the ERA5 reanalysis (Hersbach et al., 2020) and EOBS (Haylock et al.,  
 14 2008) data as references to select CMIP6 data (the selection procedure is detailed below). We  
 15 downloaded the data for the Paris area from the Climate Explorer  
 16 (<https://www.climexp.knmi.nl>).  
 17



18  
 19 *Figure 1: Ile de France Area in Western Europe (panel a). The red rectangle in panel b refers to the region that is considered in*  
 20 *the model and reanalysis data. Paris “intra-muros” is indicated in blue.*

21 In order to assess the potential role of large-scale climate variability we computed from the  
 22 CMIP6 archive:

- 23 • an El Niño 3.4 index (Trenberth, 1997) based on sea-surface temperature (SST) in the  
 24 Central Equatorial Pacific (5N-5S, 170W-120W). This index was computed from  
 25 monthly anomalies of spatial averages of SST. Positive values of the Niño3.4 index  
 26 correspond to El Niño episodes.
- 27 • An Atlantic Multi-decadal Oscillation (AMO) index (Kerr, 2005) based on SST in the  
 28 North Atlantic region. This index was computed as a spatial average (80W-0E; 0-60N)  
 29 of monthly SST. The global SST mean value was subtracted in order to remove long  
 30 term trends.

31 These two indices account for most of the interannual large scale variability of climate.



## 1 3.2 Pre-processing

2 All CMIP6 models are prone to biases, in particular due to their horizontal resolution (Carvalho  
3 et al., 2021), which leads to a misrepresentation of several processes which are relevant to  
4 reproduce the energy balance near the surface (Domeisen et al., 2023). One way to solve this  
5 issue is to use bias correction methods (Maraun and Widmann, 2018). Such an approach  
6 requires a “sound” reference, like a very high-resolution reanalysis (e.g., SAFRAN (Quintana-  
7 Segui et al., 2008)), which is not necessarily available everywhere in the world. In addition,  
8 such bias correction methods are rather computer costly, and have only been performed on  
9 a small subset of CMIP6 (e.g., only one member per model/group, for arbitrarily selected  
10 models). Finally, the bias correction of each individual simulation crunches model statistics  
11 towards the statistics of one realization of the true climate variability over a limited time  
12 period (the correction training period), the observed one, and may thus artificially reduce the  
13 simulated natural variability. This effect can be particularly exacerbated for extremes, because  
14 the interdecadal variability at regional scale can be large.

15

16 We chose here an alternative approach consisting of selecting models yielding the smallest  
17 biases over Ile de France of the “historical” simulation for TG, taking advantage of the large  
18 number of simulations available in CMIP6. We made a comparison of TG in historical CMIP6  
19 model simulations with ERA5 and EOBS between 1995 and 2014. We performed a  
20 Kolmogorov-Smirnov (k-s) test (von Storch and Zwiers, 2001) between each historical  
21 simulation, and ERA5 (and EOBS), to compare the probability distributions of daily summer  
22 TG in CMIP6 models and reanalyses or EOBS. The threshold we consider for the k-s test value  
23 is 0.1. We opted for an “inclusive” approach for model selection: the whole ensemble of one  
24 model is kept when at least one member yields a TG probability distribution between 1995  
25 and 2014 that is similar to ERA5 or EOBS.

26 There are two reasons for this strategy:

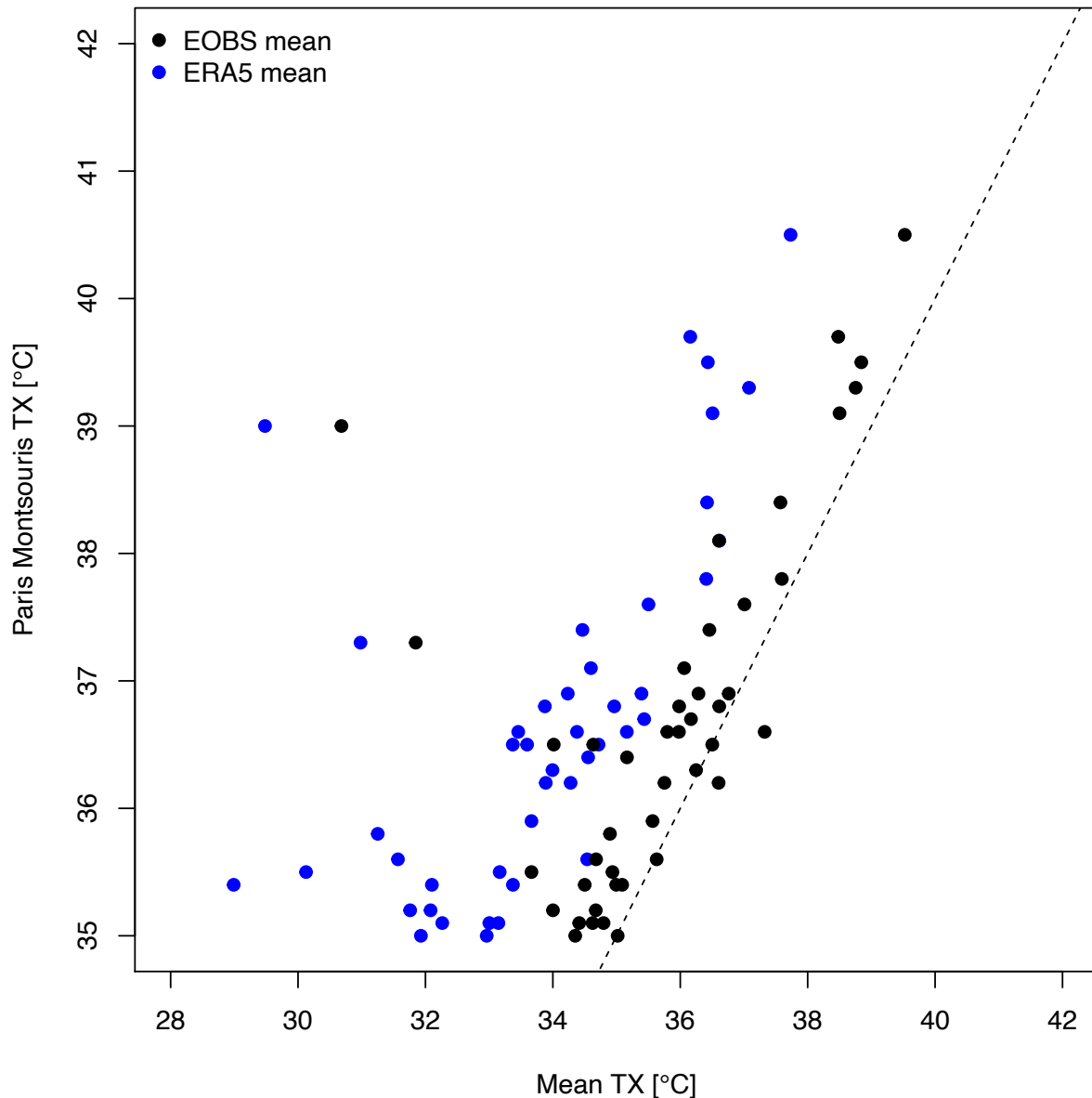
- 27 1. As stated earlier, there is a small offset between TG in ERA5 and EOBS for the Paris  
28 area, which means that ERA5 would not pass the Kolmogorov-Smirnov test if EOBS was  
29 chosen as a reference (and vice versa). There is no reason to favor EOBS over ERA5,  
30 which does not include information in Paris *intra muros* (e.g., the Paris Montsouris  
31 station), and it is reasonable to compare CMIP6 with a climate model simulation that  
32 best resembles observations, such as a reanalysis product.
- 33 2. If a CMIP6 model yields an ensemble to sample internal variability, some of its  
34 members could be different from an observation reference during a 20-year period,  
35 because model years are not “real world” years. But we do not want to reject them,  
36 because if one member is satisfactory, it suggests that the model is able to reproduce  
37 observations over a 20-year period of time, so that scenario simulations could bring  
38 relevant information. Some models come with only one run, so that this test might  
39 exclude them if this only run does not pass a statistical test with observations. This  
40 encourages large ensemble approaches, as discussed by (Bevacqua et al., 2023).

41 This selection procedure obviously contains arbitrary elements (k-s test threshold, length of  
42 time series for comparisons, period of comparison, reference data, choice of variable for  
43 comparison). In a preliminary study (in French: <https://grec-idf.eu/simulations-paris-50c/>), we  
44 used a different selection procedure (which was based on tests on TX rather than TG, and  
45 removed simulations that did not pass the test). This led to a somewhat different (smaller)  
46 ensemble of models, but the overall results in terms of first occurrence and global warming  
47 were similar. This suggests a robust behavior of this pre-processing step.

1  
2 As it is, this procedure selects 819 of the available 1288 simulations (with 585 SSP simulations),  
3 and 12 of the 26 CMIP6 models (outlined in boldface in Table 1).  
4

### 5 3.3 Selection of events

6 An event exceeding 50°C is potentially very local and short lived, with an amplification by  
7 urbanization and surface water availability. We consider a small region that averages urban  
8 areas (Paris *intra-muros*) and suburban areas with forests. Due to the urban heat island effect,  
9 we estimate that 50°C can be exceeded within Paris, when TX exceeds 48°C over the Ile-de-  
10 France area. This assumption is justified by computing the differences of TX between  
11 observation at Paris-Montsouris station, and the average over the Ile de France region (Figure  
12 2). There is a systematic offset between TX in Paris-Montsouris and the average over the Paris  
13 area when TX exceeds 35°C. Therefore, we consider that TX exceeds 50°C in Paris when TX  
14 exceeds 48°C over Ile de France. This empirical threshold could be modified. We also verified  
15 that for extreme heat days, this temperature variation is typical of intra-region variations, over  
16 the last 10 years for which we could have access to more stations (from  
17 <https://www.infoclimat.fr>).  
18  
19



1  
2 *Figure 2: Scatter plot of TX in Paris Montsouris versus the average of TX over the region outlined in Figure 1, when TX exceeds*  
3 *35°C in Paris Montsouris. The averages are computed from the EOBS (black circles) data and the ERA5 reanalysis (blue circles)*  
4 *data. The dashed line is the diagonal line.*

5  
6 From a list of 12 models and 585 simulations, we identified the years with at least one  
7 exceedance of 48°C before 2100. The results are summarized in Table 2 (not all model  
8 simulations in Table 1 reach 48°C before 2100).

9

| Model name       | Scenario      | #members with<br>TX>48°C/#Available<br>members | First year<br>with<br>TX>48°C | GMST (°C)   | GW1 (°C)   |
|------------------|---------------|--|-------------------------------|-------------|------------|
| CanESM5          | ssp370        | 12/50  | 2079                          | 18.6        | 3.5        |
| CanESM5          | ssp585        | 23/50  | 2071                          | 19.2        | 3.9        |
| <b>CMCC-ESM2</b> | <b>ssp245</b> | <b>1/1</b>                                     | <b>2077</b>                   | <b>17.3</b> | <b>2.8</b> |
| CMCC-ESM2        | ssp370        | 1/1  | 2071                          | 17.3        | 2.8        |
| <b>CMCC-ESM2</b> | <b>ssp585</b> | <b>1/1</b>                                     | <b>2049</b>                   | <b>16.7</b> | <b>2.1</b> |

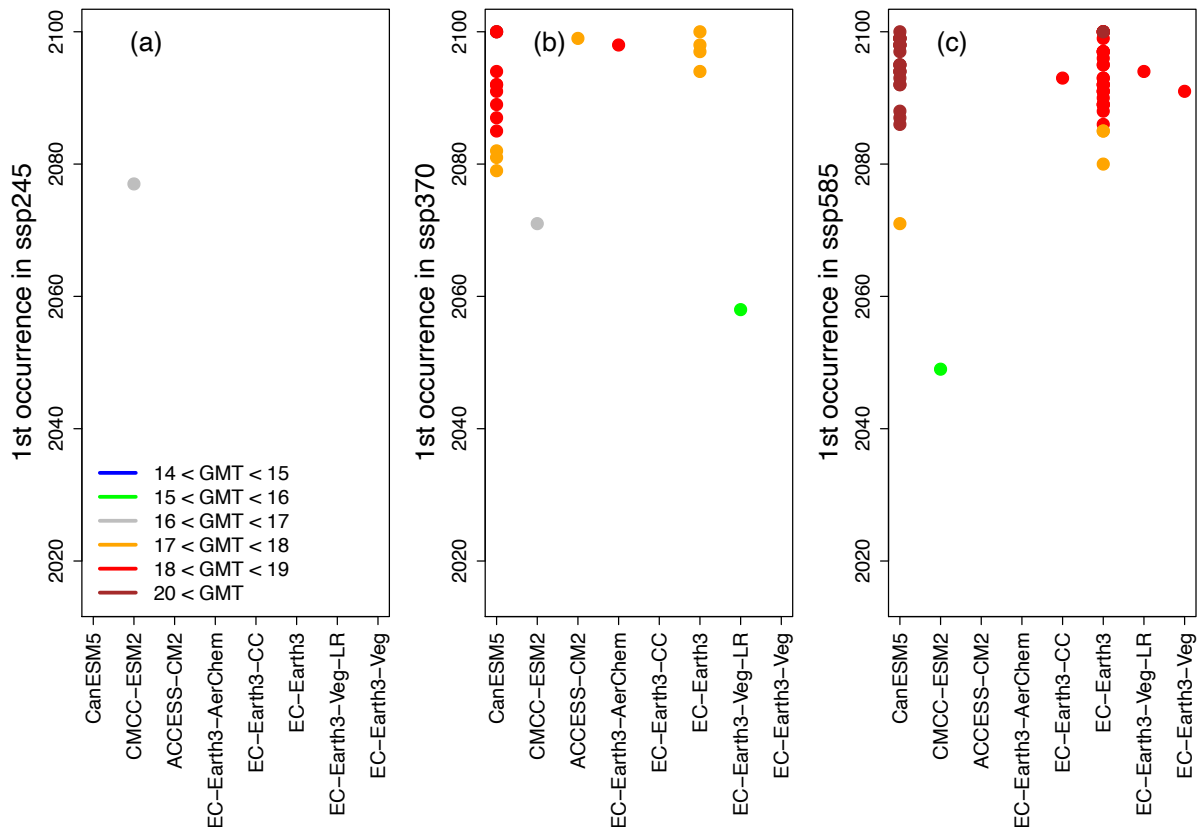
|                         |               |            |             |             |            |
|-------------------------|---------------|------------|-------------|-------------|------------|
| ACCESS-CM2              | ssp370        | 1/3        | 2099        | 18.8        | 4.1        |
| EC-Earth3-AerChem       | ssp370        | 1/1        | 2098        | 19.1        | 5.1        |
| EC-Earth3-CC            | ssp585        | 1/1        | 2093        | 19.6        | 4.9        |
| EC-Earth3               | ssp370        | 4/52       | 2094        | 18.6        | 3.4        |
| EC-Earth3               | ssp585        | 29/58      | 2080        | 18.5        | 3.5        |
| <b>EC-Earth3-Veg-LR</b> | <b>ssp370</b> | <b>1/3</b> | <b>2058</b> | <b>16.3</b> | <b>2.7</b> |
| EC-Earth3-Veg-LR        | ssp585        | 1/3        | 2094        | 19          | 5.4        |
| EC-Earth3-Veg           | ssp585        | 1/8        | 2091        | 18.9        | 4.6        |

1  
2 *Table 2: List of models with at least one simulation that exceeds 48°C in Paris at least for one day. We indicate the year of the*  
3 *first occurrence of TX>48°C among all members of the same scenario. The fifth column indicates the global surface*  
4 *temperature (GMST in °C) when the event occurs. The sixth column indicates the GMST difference (GWI, in °C) with a 1950-*  
5 *2000 baseline. The three simulations that are discussed in the results section are outlined in boldface.*

## 6 4 Results

### 7 4.1 Event occurrence in CMIP6

8 We find that 8 models, among those selected to be realistic, exceed, at least once, 48°C  
9 between 2020 and 2100. Figure 3 and Table 2 report models for which at least one member  
10 in one scenario yields a TX>48°C event. Those 8 models produced 232 simulations. Among this  
11 ensemble, 81 simulations yield at least one TX>48°C event (third column in Table 2).  
12



13  
14 *Figure 3: Time of first exceedance of 48°C in CMIP6 models for three SSP scenarios. The vertical axis indicates the year of first*  
15 *occurrence of TX>48°C in the Ile-de-France region, including Paris in model simulations. TX can exceed 48°C at later years, but*  
16 *this is not reported in the figure. The colors indicate the GMST for the 20 years around the year of TX>48°C (panel (a) for*  
17 *legend).*

18

1 We first consider the four SSP separately. For illustration purposes, we select the model  
2 simulations with the earlier dates that reach 48°C in the Paris area. We find that TX never  
3 exceeds 48°C in the SSP1-2.6 scenario. Therefore, we focus on SSP2-4.5, SSP3-7.0 and SSP5-  
4 8.5 (Figure 3). Only CMCC-ESM2 reaches the threshold with SSP2-4.5 (Figure 3a). This model  
5 was run with only one member.

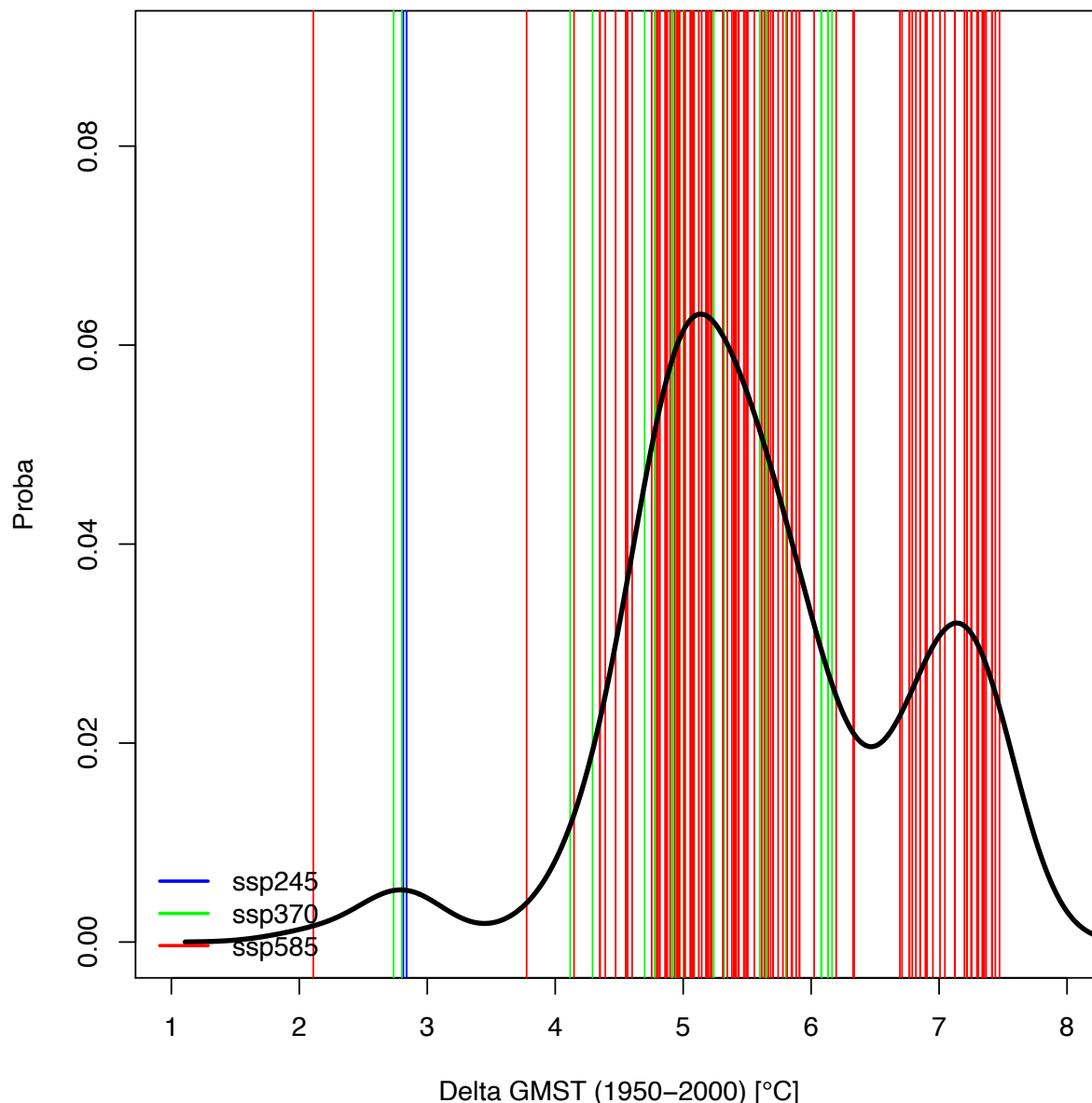
6 We computed the GMST increase (GWI) of the decades around each event since a 1950-2000  
7 baselines. From Figure 4, it appears that TX>48°C events in CMIP6 simulations occur when the  
8 GWI exceeds 2°C.

9 Most of the selected CMIP6 simulations (with 2 exceptions) do not reach this threshold as long  
10 as the GMST does not exceed 16°C (Figure 3), which correspond to a GWI of about 2.5°C since  
11 1950-2000 (Figure 4). As reaching this temperature is physically possible (Noyelle et al., 2023b;  
12 Zhang and Boos, 2023), those simulations will be discussed in this paper.

13 There is a shift of CMIP6 model behavior with SSP3-7.0, where 6 models reach the 48°C  
14 threshold between 2079 and 2100 (i.e., within the expected lifetime of the junior authors of  
15 this paper). The GWI for those models is larger than 2.7°C (with respect to a 1950-2000  
16 baseline: Figure 4).

17 With SSP5-8.5, eight models reach the 48°C threshold between 2049 and 2100, with GWI  
18 warming larger than 2.1°C (with respect to a 1950-2000 baseline). Two models (CMCC-ESM5  
19 and EC-Earth-Veg-LR) reach this threshold before 2055 (i.e., within the expected lifetime of  
20 the senior authors of this paper).

21



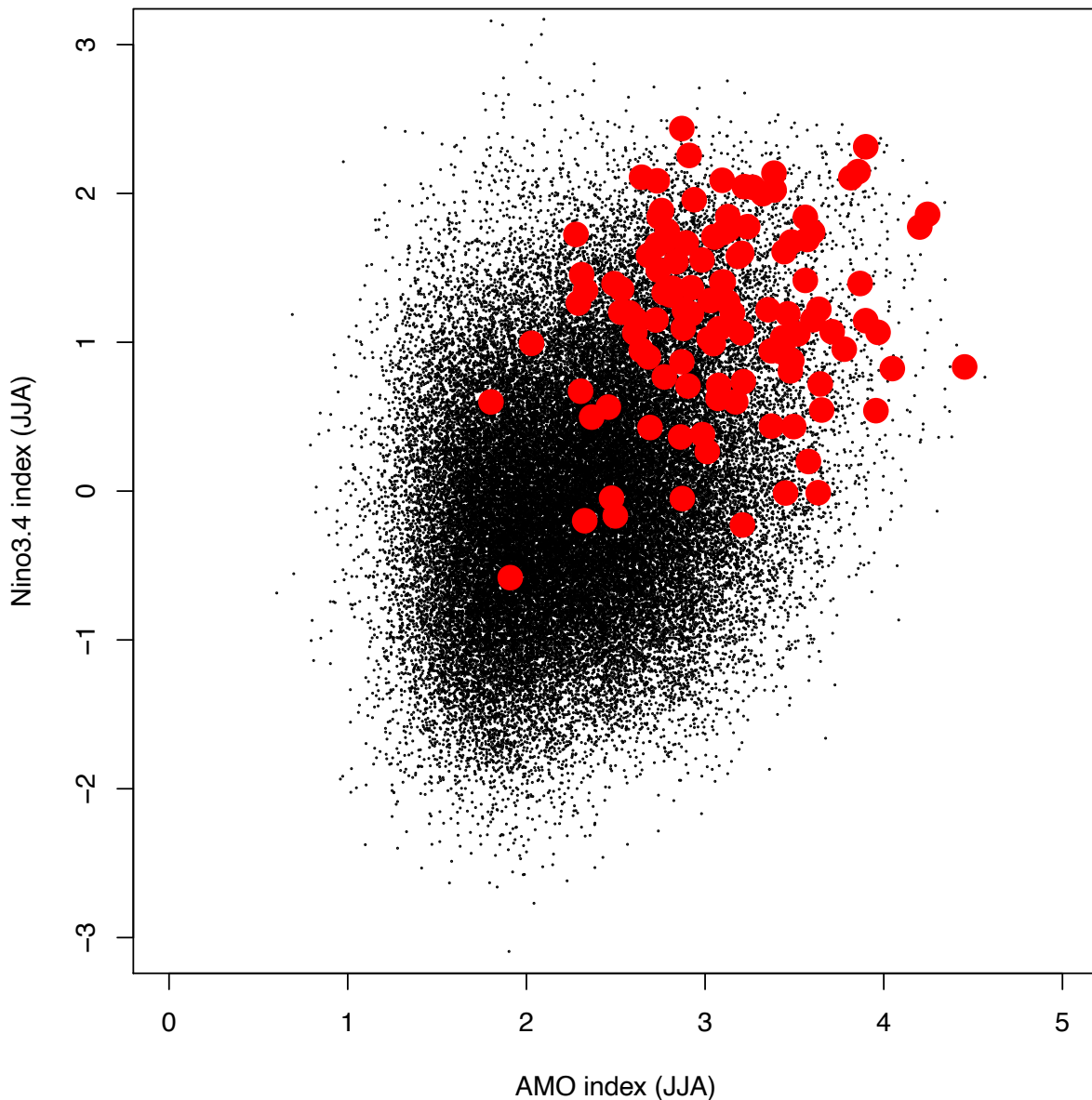
1  
 2 *Figure 4: Distributions of GMST increase (GWI) values when TX>48°C in Paris, from reference baselines of GMST in 1950-2000.*  
 3 *The vertical bars indicate all occurrences of TX>48°C. The colors indicate the SSP scenario of the TX>48°C event occurrences.*  
 4 *The black line is an empirical probability density function of the year of occurrence of TX>48°C.*

5 We pooled all 81 simulations for which TX exceeds 48°C and estimated an empirical probability  
 6 function for GWI values from a 1950-2000 baseline. The empirical probability was weighted  
 7 by the total number of considered simulations (232). This gives a crude idea of the probability  
 8 to exceed the 48°C threshold for GWI levels of warming. There are more sophisticated ways  
 9 of obtaining such probabilities, in particular using Extreme Value Theory (Coles, 2001; Robin  
 10 and Ribes, 2020). We defer such analyses to a future paper.

11 We notice in Figure 4 (black line) that a peak probability is obtained when GWI (from 1950-  
 12 2000) is around 5°C (around 6% chance). If GWI is lower than 2°C, this probability is negligible.  
 13 It becomes measurable (1% chance) when GWI reaches ~2.7°C. The reasoning behind this  
 14 statement is that one needs more than  $10^4$  years of data in order to sample events of  
 15 probability  $\approx 10^{-2}$ . With our selection procedure, we have an ensemble of  $\approx 49000$  years of  
 16 simulations. Due to the nonstationarity of the simulations, we estimate that probabilities  
 17 higher than  $\approx 10^{-2}$  can be detected.

1 4.2 Large-scale variability

2 The rationale for using ensembles from a multi-model suite of climate models was to sample  
3 large-scale climate variability. El Niño and Atlantic multi-decadal variability are major modes  
4 that are likely to affect long term variability. Niño3.4 and AMO indices were computed for the  
5 simulations of the 8 models for which TX>48°C occurs before 2100, for all scenarios.  
6 Figure 5 shows the June-July-August (JJA) averages of the two indices in all simulations  
7 (historical and scenarios). Note that the AMO index values are positive in the summer (and  
8 negative in the winter) and are not centered around 0 values.  
9



10  
11 *Figure 5: Scatter plot of Niño3.4 and AMO indices for the model simulations in Table 2, for June-July-August. The red circles*  
12 *indicate the values when a TW>48°C event occurs.*

13 We find that the TX>48°C events that are outlined in Figure 3 generally occur when the two  
14 large-scale indices are above average, i.e., during El Niño patterns and high AMO. This is  
15 consistent across the detected events, among the 8 considered climate models. North Atlantic  
16 warm temperatures indeed tend to favor a warm summer background.



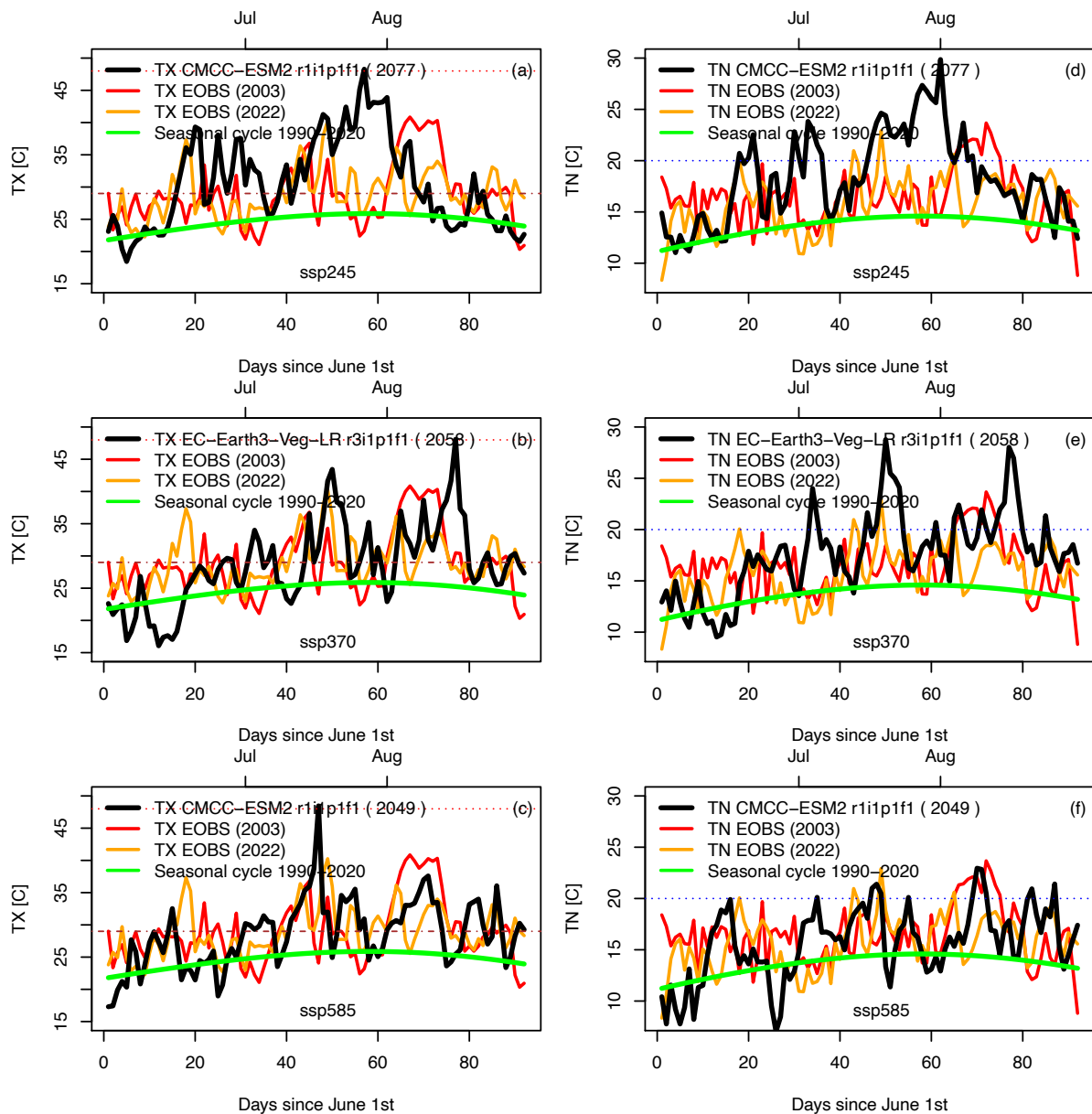
### 1 4.3 Daily summer variations for heat events

2 We select the first occurrence of  $T_X > 48^\circ\text{C}$  for each SSP scenario. We hence retain CMCC-ESM2  
3 for SSP2-4.5, EC-Earth3-Veg-LR for SSP3-7.0 and CMCC-ESM2 for SSP5-8.5 (Table 2). This  
4 choice is obviously arbitrary from the physical point of view. For illustration purposes, we will  
5 focus on the earliest occurrences, i.e., the events that the authors of this paper are likely to  
6 witness.

7 The summer time series of daily  $T_X$  and  $T_M$  (from June 1st to August 31st) are shown in Figure  
8 6 for the three selected model, along with the already experienced extremes of 2003 and  
9 2022. Apart from the  $T_X > 48^\circ\text{C}$  peaks, the distributions of temperatures are within the  
10 variations observed during the hot summers of 2003 and 2022, which shows that the whole  
11 summers are already warm. As stated in the Introduction, Météo-France defines a heatwave  
12 (“canicule”) in Paris when  $T_X$  exceeds  $31^\circ\text{C}$  and  $T_N$  exceeds  $21^\circ\text{C}$   
13 [[https://meteofrance.com/actualites-et-dossiers/comprendre-la-meteo/canicule-vague-ou-](https://meteofrance.com/actualites-et-dossiers/comprendre-la-meteo/canicule-vague-ou-pic-de-chaieur)  
14 [pic-de-chaieur](https://meteofrance.com/actualites-et-dossiers/comprendre-la-meteo/canicule-vague-ou-pic-de-chaieur)]. Such a definition depends on the region, with higher thresholds in the  
15 Southern part of France. Due to the urban effects that were identified before, we can lower  
16 such a threshold to  $29^\circ\text{C}$  for  $T_X$ , as rough estimates over the Paris region. We retain a  $20^\circ\text{C}$   
17 threshold for  $T_N$ , as it defines tropical nights.

18 We find that reaching a  $48^\circ\text{C}$  peak is obtained during warm summers (according to present-  
19 day standards: Figure 6), with a large number of days above the mean seasonal cycle. During  
20 those summers the values of  $T_X$  exceed  $29^\circ\text{C}$  and  $T_N$  exceed  $20^\circ\text{C}$  on several occasions, which  
21 means that several heatwaves (similar to those of 2003 and 2022) also occur during the course  
22 of those summers. The peaks of  $T_X > 48^\circ\text{C}$  correspond to  $T_X$  anomalies of more than  $20^\circ\text{C}$  above  
23 the present-day seasonal cycle and last for one day.

24 The selected simulations show periods of tropical nights (i.e., when the minimal daily  
25 temperature  $T_N$  exceeds  $20^\circ\text{C}$ ). We note that the warmest tropical nights do not necessarily  
26 occur on the same day as the warmest  $T_X$ , although tropical nights do occur when  $T_X$  is high.  
27



1  
2 *Figure 6: Time series of daily maximum (TX: left column) and minimum (TN: right column) temperatures in the Paris area for*  
3 *three scenarios. Black lines indicate TX and TN in models. Red and orange lines indicate TX and TN in EOBS for the summers*  
4 *of 2003 and 2022 (respectively). The horizontal red dotted line indicates the 48°C threshold for TX. The horizontal dashed*  
5 *brown lines indicate the 29°C TX threshold for heatwaves. The horizontal blue dotted line indicates 20°C (TN threshold for*  
6 *tropical nights). The green lines indicate the seasonal cycle for TX and TN, computed from the EOBS data (1990-2020).*

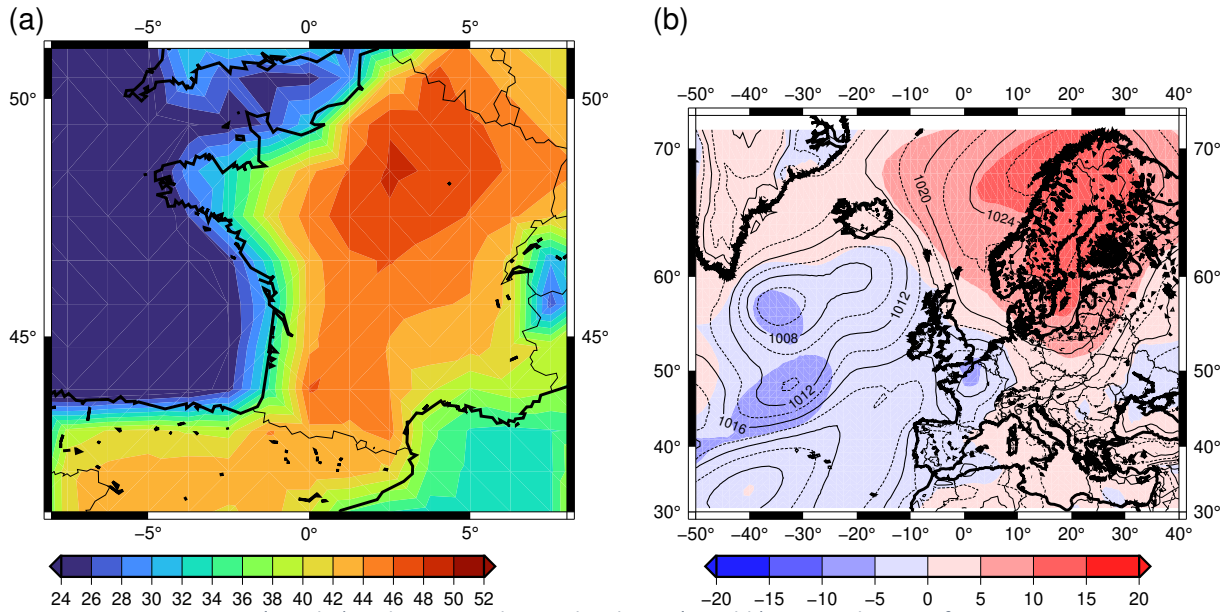
#### 7 4.4 TX and SLP patterns

8 This section serves as a quick check that the climate simulation data are “fit for purpose” and  
9 do not yield obvious errors. Systematic process studies are deferred to other papers (D’Andrea  
10 et al., 2024; Noyelle et al., 2023b, a).

11 The temperature patterns over France and the atmospheric circulation (SLP) patterns over the  
12 Eastern North Atlantic during the three events are shown in Figure 7 to Figure 9. SLP anomalies  
13 are computed with respect to the summer (June-July-August) average for each SSP scenario.  
14 For SSP2-4.5, we selected the CMCC-ESM5 model. The TX>48°C event occurs in July 2077, with  
15 a GWI of ~2.3°C. The maximum TX pattern is near the Paris region and TX exceeds 40°C over  
16 most of France (Figure 7a). Therefore, the heat event over Paris is also obtained for many  
17 gridcells of the model around the Paris region. The atmospheric circulation pattern shows an  
18 anticyclone over Scandinavia, and lows over France and west of France (Figure 7b). This

1 atmospheric pattern also corresponds to observed heatwaves of 2003 (Yiou et al., 2021) and  
 2 2022 in France (Herrera-Lormendez et al., 2023; Ibebuchi and Abu, 2023). The peaks of  
 3 temperature were reached in August 2003 and July 2022, after persisting anticyclonic  
 4 (blocking) atmospheric pattern above Scandinavia (more than 2 weeks), and drought  
 5 conditions. Such atmospheric patterns correspond to the most intense heatwaves that could  
 6 occur in the Paris area (Noyelle et al., 2023a).

7



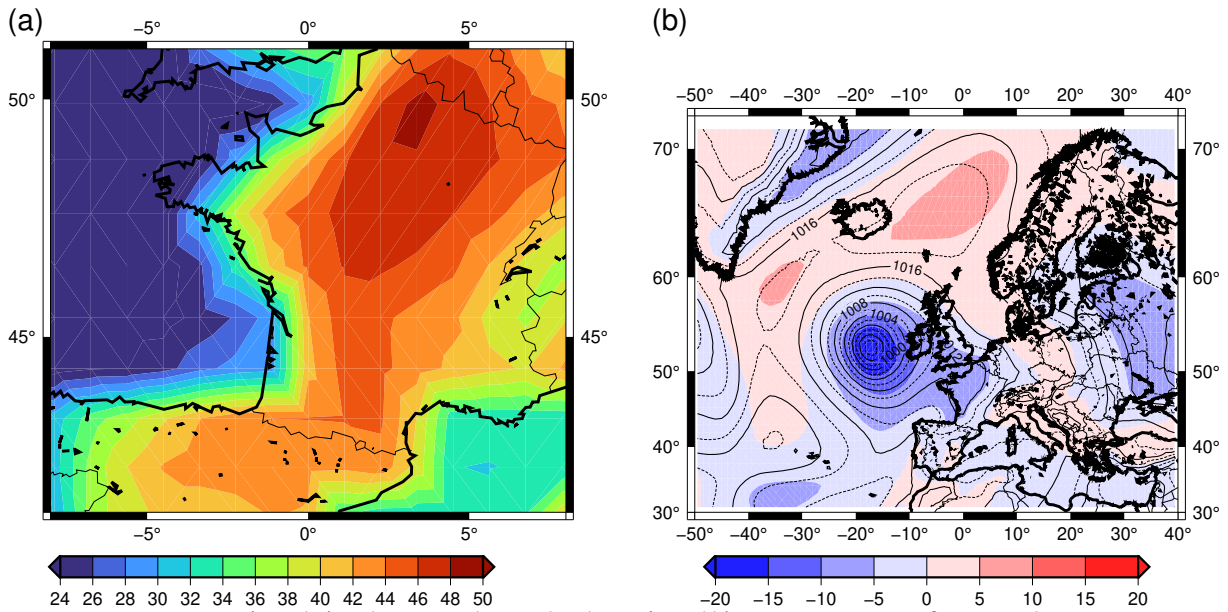
8

9

10 Figure 7: TX over France (panel a) and SLP over the North Atlantic (panel b) on 27 July 2077, for CMCC-ESM2, in SSP2-4.5  
 11 (r1i1p1f1). TX (panel a) is expressed in °C. SLP is expressed in hPa (isolines in panel b). Colors in panel (b) correspond to  
 anomalies of SLP (in hPa) with respect to the summer average.

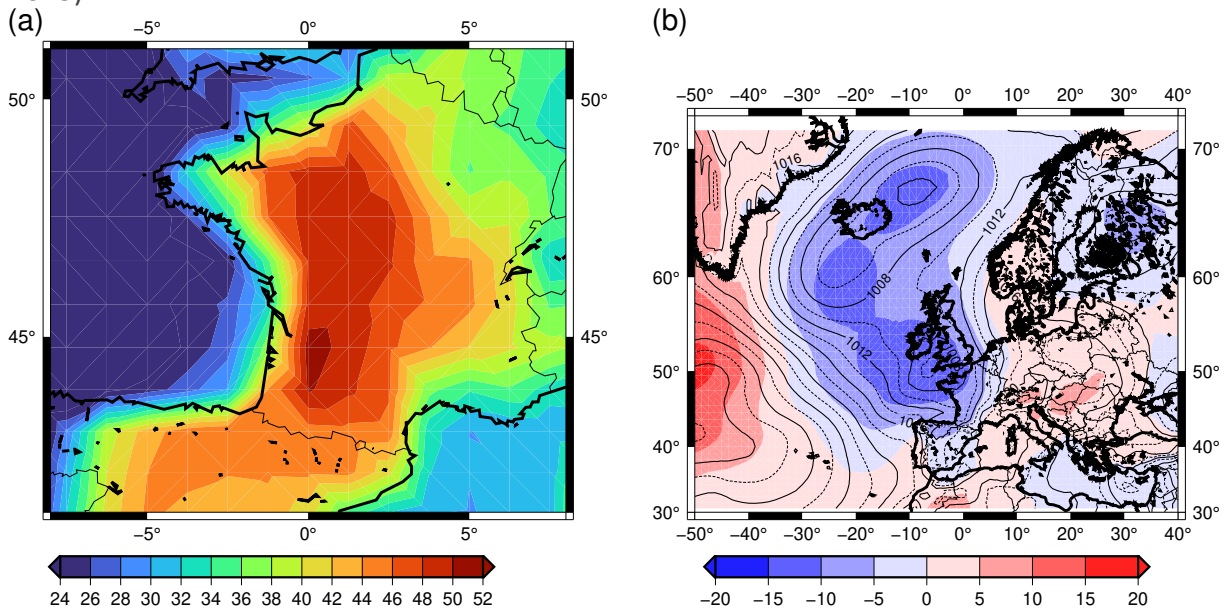
12 For SSP3-7.0, we selected the EC-Earth3-Veg-LR model. TX exceeds 48°C on the 16<sup>th</sup> of August  
 13 2077 in the r3i1p1f1 member, i.e. after the apex of the seasonal cycle. The GWI from 1950-  
 14 2000 is ~2.7°C. The center of the extreme TX pattern is located in North East France (Figure  
 15 8a). The hot pattern covers most of France, with TX values above 40°C over most of the  
 16 country. The atmospheric circulation shows an anticyclonic pattern between Iceland and  
 17 Scandinavia and in Central Europe. The circulation yields a strong cyclonic pattern west of  
 18 Ireland (Figure 8b). Such a pattern is likely to convey warm air from North Africa into France.

19



1  
2 Figure 8: TX over France (panel a) and SLP over the North Atlantic (panel b) on 16 August 2058, for EC-Earth3-Veg-LR, in SSP3-  
3 7.0 (r3i1p1f1). TX (panel a) is expressed in °C. SLP is expressed in hPa (isolines in panel b). Colors in panel (b) correspond to  
4 anomalies of SLP (in hPa) with respect to the summer average.

5  
6 For SSP5.8-5, the early TX>48°C event occurs in July 2049 in CMCC-ESM2 with a GWI of ~2.1°C  
7 (since 1950-2000). The center of the event occurs in the South West of France, with  
8 temperatures exceeding 50°C (Figure 9a). Most of the country yield TX over 42°C. Northern  
9 Spain is also affected by high temperatures. The heat does not extend to the east of France.  
10 The atmospheric circulation pattern yields an anticyclonic feature east of France (centered  
11 over the Balkans), and a depression between Iceland and Brittany (Figure 9b). In both cases,  
12 the presence of a depression on the west side of the heatwave likely increases temperature  
13 over France via southerly advection or diabatic heating in the frontal area (Domeisen et al.,  
14 2023).



15  
16 Figure 9: TX over France (panel a) and SLP over the North Atlantic (panel b) on 17 July 2049, for CMCC-ESM2, in SSP5-8.5  
17 (r1i1p1f1). TX (panel a) is expressed in °C. SLP is expressed in hPa (isolines in panel b). Colors in panel (b) correspond to  
18 anomalies of SLP (in hPa) with respect to the summer average.

1 Out of those three events (from three SSP scenarios, and three different climate models),  
2 three events occur with a GWI between 2.1°C and 2.8°C. Those three events yield atmospheric  
3 patterns that are reminiscent of already observed heatwaves in Paris, albeit with exacerbated  
4 TX values.

## 5 5 Discussion

6 This paper presents a simple approach to outline extreme temperature events in a large urban  
7 and sub-urban region surrounding (and including) Paris. The methodology is based on data  
8 inspection and does not contain any sophisticated statistical (Parey, 2008; Yiou and Jézéquel,  
9 2020) or physical (Gessner et al., 2021; Ragone et al., 2018) modelling approaches. Those  
10 results serve as a first step for further in-depth studies of extreme heatwaves.

11 Many choices have been subjective (or based on previous experience): threshold of  
12 temperature daily increments, global covariate, and general frequency of extremes. The  
13 results were obtained on the IPSL computing facility, for which a (large) subset of the  
14 simulations of CMIP6 are available. The same computations are possible with access to Earth  
15 System Grid Federation (ESGF) servers throughout the world, although they would require  
16 downloading a large amount of data.

17 We have identified events corresponding to moderate GMST increase (between 2.1 and  
18 2.8°C). Those events come with spates of tropical nights (minimum temperatures over 20°C),  
19 which would exacerbate the impacts on health of exceeding 50°C during the day. Some of the  
20 Paris events correspond to larger scale events, where temperature exceeds 50°C (e.g., in the  
21 south west of France) and large parts of the country have TX above 40°C. Therefore, a crisis in  
22 Paris would also be reflected in other regions of France, where temperatures could even be  
23 higher, especially in urban areas (in Amiens: Figure 8a; or in Bordeaux: Figure 9a). We have  
24 not quantified the probability of exceeding this high threshold, because it is rarely observed  
25 more than once in each simulation. This probability is deemed to be negligible for a global  
26 surface temperature increase lower than 2°C within the next two decades. It increases to ~1%  
27 chance if the global surface temperature increases by 2.7°C. Yet, it cannot be excluded,  
28 because Western Europe warms faster than the rest of the world (Rousi et al., 2022; Vautard  
29 et al., 2023), and temperature has already reached 48.8°C in Sicily (Southern Italy) in August  
30 2023. If global surface temperature (GMST) increases by more than 4°C since 1950-2000, the  
31 probability of such hot events increases dramatically in the CMIP6 database.

32 We have not discussed in detail the mechanisms leading to hot extremes in Paris, which is left  
33 for further studies. We have shown that the prevailing large-scale conditions during those hot  
34 events correspond to El Niño states and intense AMO. Such large-scale features tend to  
35 increase surface temperature over the northern midlatitudes (Kerr, 2005; Trenberth, 1997).  
36 This result is not surprising as it explains the “background” warm summer temperatures  
37 outlined in Figure 6.

38 Several studies have shown that the mechanisms leading to hot summer temperatures in the  
39 midlatitudes are connected to (i) adiabatic warming due to atmospheric subsistence, (ii)  
40 diabatic warming due to shortwave radiation, sensible and latent heat fluxes, and (iii)  
41 Advection of warm air from neighboring regions (Domeisen et al., 2023; Röthlisberger and  
42 Papritz, 2023). The first mechanism is linked to an anticyclonic system and explains half of the  
43 high temperature anomalies in present-day climate (Röthlisberger and Papritz, 2023). Hence,  
44 the high temperature found with the CMCC-ESM2 simulation in SSP2-4.5 is coherent with this  
45 scenario. The high temperature in the two other examples (EC-Earth3-Veg-LR, SSP3-7.0  
46 (r3i1p1f1); CMCC-ESM2, in SSP5-8.5 (r1i1p1f1)) correspond to a mechanism of warm air



1 advection, due to the strong cyclonic circulation west of France. The rather short duration of  
2 the  $T > 48^\circ\text{C}$  events in the three cases (only one day), which are followed by a strong  
3 temperature drop (albeit to still hot values) correspond to a limiting mechanisms of  
4 convection developed by (Noyelle et al., 2023b; Zhang and Boos, 2023). The verification of  
5 such mechanisms requires atmospheric data on several geopotential heights, which are not  
6 available in all CMIP6 simulations. Surface precipitation alone does not provide enough  
7 information. Hence, a systematic investigation of the physical mechanisms leading to such  
8 high temperatures, and how those mechanisms are affected by climate change, requires many  
9 “manual” verifications on the available data files, which are beyond the scope of this paper.

## 10 6 Conclusion

11 This paper aims at exploring how a temperature of  $50^\circ\text{C}$  could be reached in the Paris area, by  
12 examining the CMIP6 database. The general questions that were asked by the City of Paris  
13 where: when? what level of global warming? What type of meteorology? Exploring the CMIP6  
14 database poses a few statistical, physical and computing challenges that are tackled in the  
15 paper.

16 This paper is meant to provide an automated data-processing chain for the analysis of  
17 extremes in this simulation ensemble, with an illustration for the Paris area. This serves as a  
18 demonstrator for a climate service for policymakers, which can be transposed to other regions  
19 in the world. The important points of this data mining demonstrator are:

- 20 1. the reproducibility of the diagnostics, so that the analyses could be replicated on  
21 climate projection updates for the upcoming IPCC report,
- 22 2. the facilitated transposition to other places in the world (e.g., the City of Perpignan,  
23 France: [https://madeinperpignan.com/evenement-perpignan-50-degres-climat-eau-  
24 biodiversite/](https://madeinperpignan.com/evenement-perpignan-50-degres-climat-eau-biodiversite/)).

25 One of the salient points for decision makers of our analysis is the estimate of the probability  
26 of exceeding high temperature thresholds as a function of the global mean temperature  
27 increase. If the detection threshold is lowered to  $46^\circ\text{C}$  (which is not far from the present record  
28 in Paris:  $42.6^\circ\text{C}$  at Paris-Montsouris in 2019), more models are selected (11 vs. 8 for  $48^\circ\text{C}$ ), and  
29 the probability of exceeding this threshold for a GMST increase of  $2\text{--}4^\circ\text{C}$  since 1950-2000 is  
30 multiplied by a factor of 2 (not shown).

31 A major caveat of this automated data mining analysis is that it is necessary to check manually  
32 that the climate model simulations do not contain hard-to-detect mistakes or biases, such as  
33 the numerical instabilities of the UKESM model (but not limited to this model), which are  
34 documented in <https://errata.ipsl.fr/static/index.html> (among other official sites).

35 We do not propose a complete climate analysis of the events (which would be an entire paper  
36 by itself) and focus on extremely simple diagnostics. Hence this data-processing chain can  
37 serve as a preliminary step to identify relevant (in the sense that was defined in the methods  
38 section) simulations, and avoid sophisticated (and computer costly) steps of bias correction.

## 39 7 Acknowledgements

40 This paper was motivated by the Groupe régional d’expertise sur le changement climatique et  
41 la transition écologique (GREC) in Île-de-France. We thank the ESPRI computing mesocenter  
42 at IPSL for making the CMIP6 data available. We thank Olivier Boucher (LMD) for discussions  
43 on the choices of parameter of the computer scripts, and checking the reproducibility of the  
44 results.

## 1 8 Funding sources

2 This paper received the support of the grant ANR-20-CE01-0008-01 (SAMPRACE). This work  
3 also received support from the European Union’s Horizon 2020 research and innovation  
4 programme under grant agreement No. 101003469 (XAIDA). PY also acknowledges the  
5 support from ANDRA and EDF (grant COSTO).

## 6 9 Code and data availability

7 The codes (in R, cdo and shell scripts) to perform all data processing computations is available  
8 from <https://github.com/pascalyiou/Paris50C.git>

9 The CMIP6 data files are available from the IPSL ESGF node: [https://esgf-  
10 node.ipsl.upmc.fr/projects/esgf-ipsl/](https://esgf-node.ipsl.upmc.fr/projects/esgf-ipsl/)

11 ERA5 reanalysis and E-OBS data sets were retrieved from the Climate Explorer:  
12 <https://climexp.knmi.nl/> . We extracted tasmax and tasmin over the region outlined in Figure  
13 1, directly from the Climate Explorer.

## 14 10 Declaration of generative AI in writing

15 This manuscript was entirely written by its authors, without any use of generative AI.

## 16 11 Author contribution

17 RV and NdN initiated the study. PY drafted the manuscript and ran the computations. YR  
18 provided Figure 1. RN and FdA provided input on the analyses of the manuscript. All authors  
19 contributed to the writing of the manuscript.

## 20 12 References

21 Bador, M., Terray, L., Boe, J., Somot, S., Alias, A., Gibelin, A.-L., and Dubuisson, B.: Future  
22 summer mega-heatwave and record-breaking temperatures in a warmer France climate,  
23 *Environmental Research Letters*, 12, 074025, 2017.

24 Bastos, A., Fu, Z., Ciais, P., Friedlingstein, P., Sitch, S., Pongratz, J., Weber, U., Reichstein,  
25 M., Anthoni, P., and Arneeth, A.: Impacts of extreme summers on European ecosystems: a  
26 comparative analysis of 2003, 2010 and 2018, *Philosophical Transactions of the Royal Society*  
27 *B*, 375, 20190507, 2020.

28 Bevacqua, E., Suarez-Gutierrez, L., Jézéquel, A., Lehner, F., Vrac, M., Yiou, P., and  
29 Zscheischler, J.: Advancing research on compound weather and climate events via large  
30 ensemble model simulations, *Nature Communications*, 14, 2145, 2023.

31 Carvalho, D., Pereira, S. C., and Rocha, A.: Future surface temperatures over Europe according  
32 to CMIP6 climate projections: an analysis with original and bias-corrected data, *Climatic*  
33 *Change*, 167, 1–17, 2021.

34 Coles, S.: *An introduction to statistical modeling of extreme values*, Springer, London, New  
35 York, 208 pp., 2001.

36 Damgé, M.: Canicule : quel est le seuil d’alerte de votre département?, *Le Monde*, 19th July,  
37 2023.

38 D’Andrea, F., Duvel, J.-P., Rivière, G., Vautard, R., Cassou, C., Cattiaux, J., Coumou, D.,  
39 Faranda, D., Happé, T., Jézéquel, A., Ribes, A., and Yiou, P.: Summer Deep Depressions  
40 Increase Over the Eastern North Atlantic, *Geophysical Research Letters*, 51, e2023GL104435,  
41 <https://doi.org/10.1029/2023GL104435>, 2024.

42 Deser, C., Terray, L., and Phillips, A. S.: Forced and internal components of winter air  
43 temperature trends over North America during the past 50 years: Mechanisms and implications,  
44 *Journal of Climate*, 29, 2237–2258, 2016.



1 Domeisen, D. I., Eltahir, E. A., Fischer, E. M., Knutti, R., Perkins-Kirkpatrick, S. E., Schär, C.,  
2 Seneviratne, S. I., Weisheimer, A., and Wernli, H.: Prediction and projection of heatwaves,  
3 *Nature Reviews Earth & Environment*, 4, 36–50, 2023.

4 Eyring, V., Bony, S., Meehl, G. A., Senior, C. A., Stevens, B., Stouffer, R. J., and Taylor, K.  
5 E.: Overview of the Coupled Model Intercomparison Project Phase 6 (CMIP6) experimental  
6 design and organization, *Geoscientific Model Development*, 9, 1937–1958, 2016.

7 Fischer, E. M., Sippel, S., and Knutti, R.: Increasing probability of record-shattering climate  
8 extremes, *Nature Climate Change*, 11, 689–695, 2021.

9 Fischer, E. M., Beyerle, U., Bloin-Wibe, L., Gessner, C., Humphrey, V., Lehner, F.,  
10 Pendergrass, A. G., Sippel, S., Zeder, J., and Knutti, R.: Storylines for unprecedented heatwaves  
11 based on ensemble boosting, *Nature Communications*, 14, 4643, 2023.

12 Florentin, A. and Lelievre, M.: Mission d’information et d’évaluation du Conseil de Paris Paris  
13 à 50 degrés : s’adapter aux vagues de chaleur, Paris City Council, 2023.

14 Gessner, C., Fischer, E. M., Beyerle, U., and Knutti, R.: Very rare heat extremes: quantifying  
15 and understanding using ensemble re-initialization, *Journal of Climate*, 1–46, 2021.

16 Haylock, M. R., Hofstra, N., Tank, A. M. G. K., Klok, E. J., Jones, P. D., and New, M.: A  
17 European daily high-resolution gridded data set of surface temperature and precipitation for  
18 1950–2006, *J. Geophys. Res. - Atmospheres*, 113, doi:10.1029/2008JD010201, 2008.

19 Herrera-Lormendez, P., Douville, H., and Matschullat, J.: European summer synoptic  
20 circulations and their observed 2022 and projected influence on hot extremes and dry spells,  
21 *Geophysical Research Letters*, 50, e2023GL104580, 2023.

22 Hersbach, H., Bell, B., Berrisford, P., Hirahara, S., Horányi, A., Muñoz-Sabater, J., Nicolas, J.,  
23 Peubey, C., Radu, R., and Schepers, D.: The ERA5 global reanalysis, *Quat. J. Roy. Met. Soc.*,  
24 146, 1999–2049, 2020.

25 Ibebuchi, C. C. and Abu, I.-O.: Characterization of temperature regimes in Western Europe, as  
26 regards the summer 2022 Western European heat wave, *Climate Dynamics*, 61, 3707–3720,  
27 2023.

28 IPCC: Climate Change 2021: The Physical Science Basis. Contribution of Working Group I to  
29 the Sixth Assessment Report of the Intergovernmental Panel on Climate Change, , In Press,  
30 <https://doi.org/10.1017/9781009157896>, 2021.

31 Kalnay, E., Kanamitsu, M., Kistler, R., Collins, W., Deaven, D., Gandin, L., Iredell, M., Saha,  
32 S., White, G., Woollen, J., Zhu, Y., Chelliah, M., Ebisuzaki, W., Higgins, W., Janowiak, J.,  
33 Mo, K., Ropelewski, C., Wang, J., Leetmaa, A., Reynolds, R., Jenne, R., and Joseph, D.: The  
34 NCEP/NCAR 40-year reanalysis project, *Bull. Amer. Met. Soc.*, 77, 437–471, 1996.

35 Kerr, R. A.: Atlantic Climate Pacemaker for Millennia Past, *Decades Hence?*, *Science*, 309,  
36 2005.

37 Maraun, D. and Widmann, M.: Statistical downscaling and bias correction for climate research,  
38 Cambridge University Press, 2018.

39 Noyelle, R., Yiou, P., and Faranda, D.: Investigating the typicality of the dynamics leading to  
40 extreme temperatures in the IPSL-CM6A-LR model, *Clim Dyn*,  
41 <https://doi.org/10.1007/s00382-023-06967-5>, 2023a.

42 Noyelle, R., Zhang, Y., Yiou, P., and Faranda, D.: Maximal reachable temperatures for Western  
43 Europe in current climate, *Environ. Res. Lett.*, 18, 094061, <https://doi.org/10.1088/1748-9326/acf679>, 2023b.

44 Parey, S.: Extremely high temperatures in France at the end of the century, *Climate Dynamics*,  
45 30, 99–112, <https://doi.org/DOI 10.1007/s00382-007-0275-4>, 2008.

46 Philip, S. Y., Kew, S. F., van Oldenborgh, G. J., Anslow, F. S., Seneviratne, S. I., Vautard, R.,  
47 Coumou, D., Ebi, K. L., Arrighi, J., Singh, R., van Aalst, M., Pereira Marghidan, C., Wehner,  
48 M., Yang, W., Li, S., Schumacher, D. L., Hauser, M., Bonnet, R., Luu, L. N., Lehner, F., Gillett,  
49 N., Tradowsky, J. S., Vecchi, G. A., Rodell, C., Stull, R. B., Howard, R., and Otto, F. E. L.:

1 Rapid attribution analysis of the extraordinary heat wave on the Pacific coast of the US and  
2 Canada in June 2021, *Earth Syst. Dynam.*, 13, 1689–1713, [https://doi.org/10.5194/esd-13-](https://doi.org/10.5194/esd-13-1689-2022)  
3 1689-2022, 2022.

4 Quintana-Segui, P., Le Moigne, P., Durand, Y., Martin, E., Habets, F., Baillon, M., Canellas,  
5 C., Franchisteguy, L., and Morel, S.: Analysis of near-surface atmospheric variables: Validation  
6 of the SAFRAN analysis over France, *Journal of applied meteorology and climatology*, 47, 92–  
7 107, 2008.

8 Ragone, F., Wouters, J., and Bouchet, F.: Computation of extreme heat waves in climate models  
9 using a large deviation algorithm, *Proc. Nat. Acad. Sci.*, 115, 24–29, 2018.

10 Riahi, K., Van Vuuren, D. P., Kriegler, E., Edmonds, J., O’neill, B. C., Fujimori, S., Bauer, N.,  
11 Calvin, K., Dellink, R., and Fricko, O.: The Shared Socioeconomic Pathways and their energy,  
12 land use, and greenhouse gas emissions implications: An overview, *Global environmental*  
13 *change*, 42, 153–168, 2017.

14 Robin, Y. and Ribes, A.: Nonstationary extreme value analysis for event attribution combining  
15 climate models and observations, *Advances in Statistical Climatology, Meteorology and*  
16 *Oceanography*, 6, 205–221, 2020.

17 Röthlisberger, M. and Papritz, L.: Quantifying the physical processes leading to atmospheric  
18 hot extremes at a global scale, *Nature Geoscience*, 16, 210–216, 2023.

19 Rousi, E., Kornhuber, K., Beobide-Arsuaga, G., Luo, F., and Coumou, D.: Accelerated western  
20 European heatwave trends linked to more-persistent double jets over Eurasia, *Nature*  
21 *communications*, 13, 1–11, 2022.

22 von Storch, H. and Zwiers, F. W.: *Statistical Analysis in Climate Research*, Cambridge  
23 University Press, Cambridge, 2001.

24 Trenberth, K. E.: The definition of El Niño, *Bulletin of the American Meteorological Society*,  
25 78, 2771–2778, 1997.

26 Vautard, R., Cattiaux, J., Hap  , T., Singh, J., Bonnet, R., Cassou, C., Coumou, D., D’Andrea,  
27 F., Faranda, D., Fischer, E., Ribes, A., Sippel, S., and Yiou, P.: Heat extremes in Western  
28 Europe increasing faster than simulated due to atmospheric circulation trends, *Nature*  
29 *Communications*, 14, 6803, <https://doi.org/10.1038/s41467-023-42143-3>, 2023.

30 Yin, J., Gentine, P., Slater, L., Gu, L., Pokhrel, Y., Hanasaki, N., Guo, S., Xiong, L., and  
31 Schlenker, W.: Future socio-ecosystem productivity threatened by compound drought–  
32 heatwave events, *Nature Sustainability*, 6, 259–272, 2023.

33 Yiou, P. and J  z  quel, A.: Simulation of extreme heat waves with empirical importance  
34 sampling, *Geosci. Model Dev.*, 13, 763–781, <https://doi.org/10.5194/gmd-13-763-2020>, 2020.

35 Yiou, P., Faranda, D., Thao, S., and Vrac, M.: Projected Changes in the Atmospheric Dynamics  
36 of Climate Extremes in France, *Atmosphere*, 12, <https://doi.org/10.3390/atmos12111440>, 2021.

37 Zhang, Y. and Boos, W. R.: An upper bound for extreme temperatures over midlatitude land,  
38 *Proceedings of the National Academy of Sciences*, 120, e2215278120, 2023.

39